Journal of Innovative Optical Health Sciences
Vol. 1, No. 2 (2008) 239–256

World Scientific
www.worldscientific.com

IN VIVO MAPPING BRAIN MICROCIRCULATION BY LASER SPECKLE CONTRAST IMAGING: A MAGNETIC RESONANCE PERSPECTIVE OF THEORETICAL FRAMEWORK

ZHENG WANG

Center for Functional and Metabolic Mapping
Robarts Research Institute

Department of Medical Biophysics
The University of Western Ontario, London, Canada
wzheng@imaging.robarts.ca

The fundamental limitations of most vascular-based functional neuroimaging techniques are placed by the fact how fine the brain regulates the blood supply system. *In vivo* mapping of the cerebral microcirculation with high resolution and sensitivity hence becomes unprecedentedly compelling. This paper reviews the theoretical background of the laser speckle contrast imaging (LSCI) technique and attempts to present a complete framework stemming from a simple biophysical model. Through the sensitivity analysis, more insights into the tool optimization are attained for *in vivo* applications. Open questions of the technical aspects are discussed within this unified framework. Finally, it concludes with a brief perspective of future research in a way analogous to the magnetic resonance imaging (MRI) technique. Such exploration could catalyze their development and initiate a technological fusion for precise assessment of blood flow across various spatial scales.

Keywords: Laser speckle contrast imaging; brain microcirculation; functional neuroimaging; magnetic resonance imaging.

1. Introduction

It has been well known that the brain requires extremely sensitive and efficient control of blood flow because there is no local energy reserve in the cortical tissue. Local increases in blood flow result from the rapid dilation of arterioles and capillaries of a restricted area in response to an episode of high neuronal activity.[1,2] Thus, variations in local cerebral blood flow (CBF) evoked by functional activation is often regarded as an indirect indicator of the changes in cortical neuronal activities.[3] This is the fundamental assumption that forms the basis of modern functional brain imaging. However, the coupling relationship between neuronal activity, oxygen/glucose metabolism, and hemodynamic responses has not been completely understood at various spatial scales.[4,5] Recently, it is known that the spatial distribution of the vascular-based hemodynamic signal was closely affected

by the anatomic geometry of the activated cerebrovascular network.[6] For example, both the arterial supply and the capillary network in the cortex contain various flow-control structures to measure up to the fluctuation of the energy demands. Therefore, it is necessary to image spatial distribution of CBF from single capillary to local vascular network (namely, achieving both high resolution and large field-of-view). Moreover, studies on the regulation mechanisms of cerebral perfusion at the local, cellular, and molecular levels will shed more light on the accurate interpretation of functional imaging results.

To address these scientific questions, one has to count on the technological development of flow measurements. After the leading work done by Kety and Schmidt in 1945,[7] there has been an explosion of techniques to study cerebral circulation across diversified spatial or temporal scales. In functional imaging field, the advances of the measurements in CBF are too many to be cited here completely, such as computerized tomography (CT), positron emission tomography (PET), functional magnetic resonance imaging (fMRI) including arterial spin labeling, phase-contrast and other derivative methods, ultrasound, laser Doppler, laser speckle, and two-photon microscopy. And, it is certain that newer techniques will be developed in the future.

Among these available techniques, optical methods are the perfect candidates that possess such capability of imaging blood flow with superior spatial/temporal resolution. However, their *in vivo* applications are largely bounded by the head, skull, and skin since the visible light cannot penetrate through it. To circumvent this problem, the cranial window technique, which has first invented in the 19th century to examine the morphology of pial vessels, is often applied. Basically, it opens a transparent window on the brain and, meanwhile, maintains an environment for the pial vessels as close to the normal one as possible with respect to intracranial pressure, composition of the surrounding fluid, and prevailing gas tensions.[8] Moreover, this transparent window allows us to make better use of optical imaging techniques because the penetration depth of optical detection was greatly improved. Besides this, it offers a sufficiently large field-of-view to visualize highly heterogeneous microcirculation network. This method provides us a great opportunity in combination with optical methods to directly observe and study the cerebral microcirculation in both acute and chronic experiments.

Laser speckle contrast imaging (LSCI) is one kind of optical imaging techniques that enables us to map real-time changes of blood flow over a relatively large area with sub-millimeter spatial resolution. It can ideally bridge the research gap between single capillary level and local cerebrovasculature network. This method has absorbed an increasing interest as an alternative approach to investigate CBF activities with regard to neural mechanisms of brain events.[9–13] This review starts from the theoretical background of this technique, and describes a biophysical model of the flow-detection process. A complete framework of LSCI is presented. Then, the sensitivity analysis of this model is derived to give more insights into its advantages and limitations. Some current technical issues are discussed in this unified

framework, particularly as an analog of magnetic resonance imaging (MRI). Finally, this paper concludes with a brief perspective of future research.

2. Theoretical Framework of LSCI

Laser speckle forms when laser light falls on an optical rough surface such as paper or the wall of a laboratory. It is of high-contrast, fine-scale granular (salt-and-peppery) pattern, which is caused by random phases interferences.[14] Speckle is also observed when laser light is transmitted through stationary diffusers or when light is scattered from particle suspensions (like erythrocytes in the perfused tissue). In fact, the speckle phenomena have analog in other fields as well, such as radar detection and ultrasonic imaging.

Whenever there is any relative movement of the surface and the observer, the speckle pattern appears to scintillate. Such randomly fluctuating speckle patterns have been studied extensively as "time-varying speckle" or "dynamic speckle",[15] which is frequently observed when biological samples are illuminated under laser light. Various aspects of properties of dynamic speckles have been exploited to measure the velocity of a moving object ever since the laser speckle theory was introduced more than 40 years ago.[14] Based on statistical definition, they are simply classified into 4 categories: the time-sequential intensity detection method (for example, zero-crossing technique[16]); the autocorrelation detection method (autocorrelation function of speckle intensity itself); the cross-correlation method (correlation function of speckle intensity at two distinct points) and the variance method, which detects the second-order moment of temporally integrated speckle-intensity distribution.

The imaging technique discussed in this paper belongs to the last category, which was first proposed by Fercher and Briers to non-contact image of the skin blood flow in 1981.[17] Among the fundamental quantities characterizing the statistics of integrated intensity variations of speckles, the LSCI method uses only their mean and standard deviation in order to determine the velocity of the moving subject. Goodman has coined an extremely important parameter — speckle contrast — as the ratio of the standard deviation to the mean intensity,[18] which was later found to be modulated by the motion of scattering particles. Therefore, we start from the speckle contrast which is of fundamental importance in relating the statistics of the detected intensity and relative change in blood flow. Note that the complete laser speckle theory can fill books by itself.[19,20] Here, only the facts that are relevant to the derivation of LSCI are re-capitulated.

Based on Goodman's results on mean and variance of integrated intensity,[19] we have the first moment $\overline{I_T}$ and variance $\sigma^2_{I_T}$ of the integrated intensity I_T measured within finite-time integral interval, T, as follows:

$$\overline{I_T} = \int_{-T/2}^{-T/2} \overline{I} d\xi = \overline{I} \cdot T \tag{1}$$

$$\sigma_{I_T}^2 = \iint_{-T/2}^{-T/2} \overline{I(\xi)I(\eta)} d\xi d\eta - (\overline{I_T})^2$$
$$= \iint_{-T/2}^{-T/2} \Gamma_I(\xi - \eta) d\xi d\eta - (\overline{I_T})^2 \quad (2)$$

where $\overline{I}$ is the mean intensity of the speckle pattern, and the function Γ_I is the statistical autocorrelation function of the instantaneous intensity. Assuming the finite-time integral as a statistical stationary process, Eq. (2) then becomes:

$$\sigma_{I_T}^2 = T \int_{-\infty}^{\infty} \left(1 - \frac{|\tau|}{T}\right) \Gamma_I(\tau) d\tau - (\overline{I_T})^2 \quad (3)$$

where the function $\left(1 - \frac{|\tau|}{T}\right)$ is the deterministic autocorrelation function of the integration window. Actually, the correlation function Γ_I is equivalent to a fourth-order coherence function of the underlying fields. Since the measured speckle data in LSCI is in terms of intensity, it is necessary to convert the autocorrelation of the electric field in the above equation to the autocovariance function of the intensity speckle pattern. Thus, the Siegert's relation can be applied here to conveniently relate them together[21]:

$$\Gamma_I(\tau) = (\overline{I})^2 [1 + |\mu_A(\tau)|^2] \quad (4)$$

where $\mu_A(\tau)$ is the normalized autocovariance of the temporal fluctuations in the intensity of a single speckle. The Siegert's relation results from many statistically independent contributions to the field at a point in space due to the scattering from a rough surface. Within a speckle pattern, many independent correlation-scattered wavefields contribute to the random walk that generates speckle. It results in the summed intensity varying from completely dark or intensely bright, which is determined by the relative phases of the various components of the sum.[18] The extreme situation is that the pattern appears completely bright or dark when either constructive or destructive inference dominates the sum.

It is worthy to mention that there are two issues to be considered. One is that the speckle pattern observed in many practical situations is effectively spatially and temporally stationary in the statistical sense.[20] The above relationship is, therefore, valid for temporal integration too. Another is that an assumption of fully developed speckle is granted when the Siegert's relation is applied in Eq. (4). It might be compromised under some circumstances.[22,23] Essentially, laser speckle is a random phenomenon that is the result of many additive and independent random events. With regard to the central limit theorem, Gaussian statistics play a fundamental role in the statistical analysis of this type of physical observation. In LSCI, we are interested in studying the statistical properties of the time-varying speckle-intensity variation caused by the complex behavior of the red blood cells (RBCs) in the vasculature network.[24] Hence, we restrict our attention to Gaussian speckle patterns for the sake of simplicity.

In LSCI, a temporal-integrated speckle pattern with respect to the exposure time, T, of the CCD detector can be obtained by substituting Eq. (4) in Eq. (3):

$$\sigma_{I_T}^2(T) = \frac{\overline{I}^2(T)}{T} \int_{-T}^{T} \left(1 - \frac{|\tau|}{T}\right) |\mu_A(\tau)|^2 d\tau \tag{5}$$

Re-call the definition of speckle contrast,

$$C = \sqrt{\frac{\sigma_{I_T}^2(T)}{\overline{I}^2(T)}} = \sqrt{\frac{2}{T} \int_0^T \left(1 - \frac{\tau}{T}\right) |\mu_A(\tau)|^2 d\tau} \tag{6}$$

Obviously, this expression of the speckle contrast is different from the one originally used by Fercher and Briers (see Eq. (8)).[17] Consequences of this discrepancy have been further explored elsewhere.[13]

Still there is no straightforward connection between the velocity we desired to know and the parameters we measured in the experiments. In principle, it is somehow possible to recover the cell-speed distribution from the measured contrast of the speckle pattern if the specific profile of $|\mu_A(\tau)|^2$ is known.[25] Concerning the complicacy of the biological system, we begin with a simple biophysical model in which the red blood cells move in the vessels to one direction with a uniform velocity distribution. The laser light shines on the stationary tissue at right angle. In this way, we can adopt Goodman's result on the expression of $\mu_A(\tau)$ as follows (the detailed derivation can be found):

$$\mu_A(\tau) = \frac{\displaystyle\iint_{-\infty}^{\infty} \left[\exp\left(\sigma^2 e^{-\frac{\Delta x^2 + \Delta y^2}{r_o^2}}\right) - 1\right] \left[\exp\left(\sigma^2 e^{-\frac{(\Delta x - v\tau)^2 + \Delta y^2}{r_o^2}}\right) - 1\right] d\Delta x d\Delta y}{\displaystyle\iint_{-\infty}^{\infty} \left[\exp\left(\sigma^2 e^{-\frac{\Delta x^2 + \Delta y^2}{r_o^2}}\right) - 1\right]^2 d\Delta x d\Delta y} \tag{7}$$

where σ^2 is the variance of the phase process; r_o^2 is the coherent radius; v is the speed of moving object and $\Delta x, \Delta y$ is spatial locations.[20] In Eq. (7), σ^2 is the dominating parameter that determines the decaying slope of $\mu_A(\tau)$. It thereby is critical to appropriately estimate the variance of the phase process. It has been known that there is a family of phase functions such as the Henyey–Greenstein (HG) function that can be well suited to describe single-scattering event in turbid media-like tissue.[26] If the deflection angle in the HG function were assumed to distribute randomly within the range 0 and π, then the variance of the phase process in the grey matter would approximate around 34π (anisotropy factor $g = 0.94$).

Then, a numerical integration in the above Eq. (7) can be obtained to get an approximate expression for $\mu_A(\tau)$ and it closely approximates to the Gaussian function.[13] When the standard deviation of phase process increases, $\mu_A(\tau)$ will abruptly converge to zero.[20] In this case, any specific profile of $\mu_A(\tau)$ such as negative exponential or Gaussian function will not make a significant difference.[19]

While the velocity v increases if assumed other parameters were fixed, the value of $\mu_A(\tau)$ will accordingly decrease such that the speckle contrast C reduces too. This inverse relationship between the velocity and speckle contrast is in agreement with previous studies,[17,27,28] suggesting that the above model is a fair resort at current stage. Nevertheless, it needs a lot of further refinements. The fact is that particles (mainly as erythrocytes) move in the blood vessels with a variety of velocities, which depends on the geometrical distribution of the cerebrovasculature and regulated by many kinds of chemical and/or neurogenic factors.[29]

If the negative exponential function is used to approximate $\mu_A(\tau)$, a simple mathematical expression for the speckle contrast is obtained as a function of the integral time T and the correlation time τ_c.

$$C = \frac{\sigma_s}{\langle I \rangle} = \left[\frac{2}{T} \int_0^T \left(1 - \frac{\tau}{T}\right) \exp(-2\tau/\tau_c) d\tau \right]^{1/2}$$
$$= \left\{ \frac{\tau_c}{T} + \frac{1}{2} \left(\frac{\tau_c}{T}\right)^2 [\exp(-2T/\tau_c) - 1] \right\}^{1/2} \quad (8)$$

From Bonner and Nossal's theory,[30] the correlation time (i.e., the decay time of the photon autocorrelation function) is inversely related to the mean translational speed of the moving blood cells. At this point, a complete theoretical framework of LSCI is constructed, as illustrated in the following flow chart (Fig. 1). Needless to say, it readily demonstrates how to decode the velocity information hidden in the statistics of the speckle images recorded by the CCD sensor.

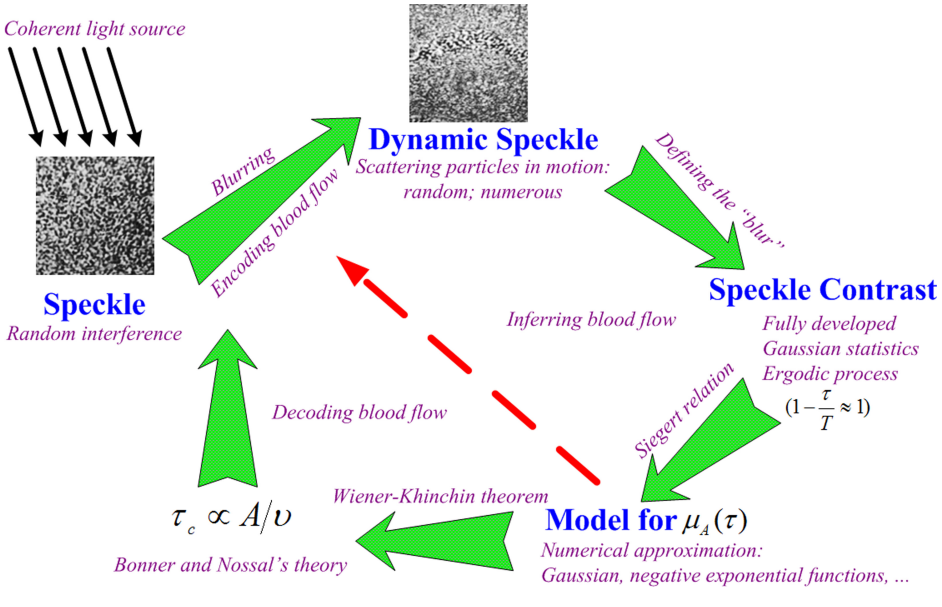

Fig. 1. Illustration of theoretical framework of LSCI.

3. Sensitivity Analysis

For the biological applications, the decay time of photon autocorrelation functions measured for capillary flow typically is of the order of 0.1 millisecond $\sim$ 1 millisecond.[30] A plot of Eq. (8) shows the relationship among these three parameters (C, T, τ_c) while the integral time, T, was set in a range from 1.0 millisecond $\sim$ 100 milliseconds in most of LSCI applications (as shown in Fig. 2). As we know about the dynamic systems, it is important to characterize the variation in the solution with respect to the variation in the values of the system parameters. Therefore, the sensitivity function of a parameter τ_c or T can be calculated from Eq. (8):

$$S(T) = \left|\frac{\partial C(\tau_c, T)}{\partial T}\right| = \left|-\frac{\sqrt{2}\tau_c}{2T^2}\frac{[T - \tau_c + (T + \tau_c)\exp(-2T/\tau_c)]}{[\tau_c^2\exp(-2T/\tau_c) + 2T\tau_c - \tau_c^2]^{1/2}}\right| \tag{9}$$

$$S(\tau_c) = \left|\frac{\partial C(\tau_c, T)}{\partial \tau_c}\right| = \frac{\sqrt{2}}{2T}\frac{[T - \tau_c + (T + \tau_c)\exp(-2T/\tau_c)]}{[\tau_c^2\exp(-2T/\tau_c) + 2T\tau_c - \tau_c^2]^{1/2}} \tag{10}$$

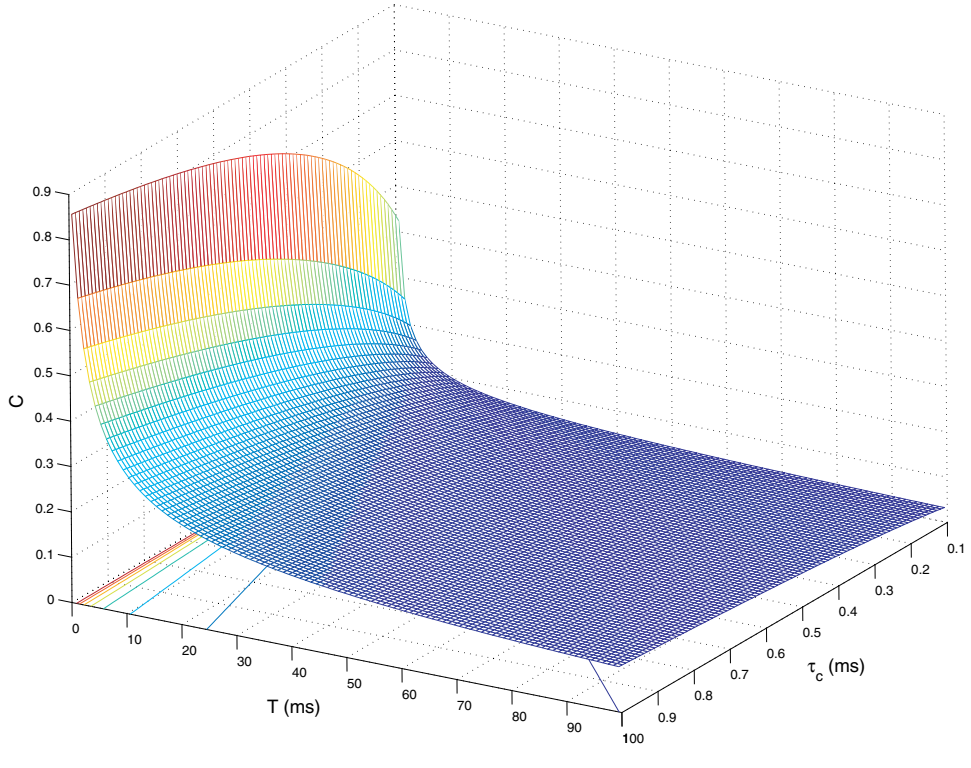

Fig. 2. A 3D plot of Eq. (8) was applied to illustrate the relationship between the correlation time τ_c, exposure time T, and speckle contrast C for theoretical model. The determination of each parameter was based on previous studies (see details in text).

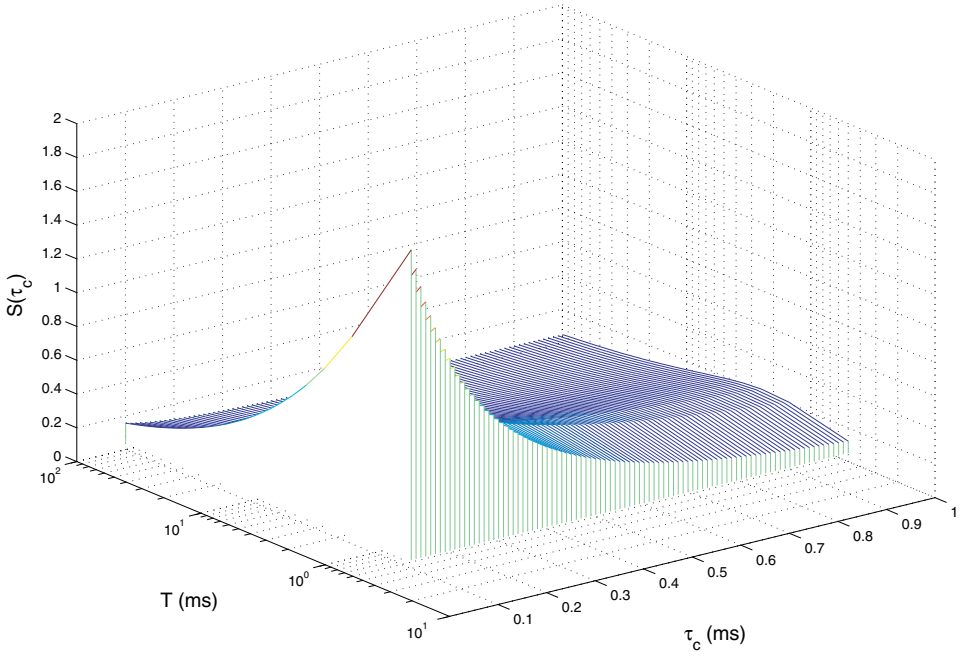

Fig. 3. Theoretical sensitivity function of parameter τ_c. At a fixed exposure time, different correlation times almost have the same sensitivity in contributing to the changes of the speckle contrast. This characteristic is kept constant while the range of exposure time is set between 1.0 millisecond and 100 milliseconds.

With the ranges of τ_c and T set same as above, Figs. 3 and 4 can be conveniently produced from Eqs. (9) and (10), respectively. Figure 3 demonstrates the feasibility of speckle imaging over a relatively large region. As mentioned above, regional CBF exhibits a significant degree of spatial heterogeneity, not only at the microscopic but also at the gross anatomical level.[29] Moreover, the regulation of local CBF across markedly different levels of functional neural units could independently vary with time in altered functional states.[31] Within the large field-of-view provided by LSCI, it is most likely to contain different correlation times at discrete levels of cerebrovascular network. From Fig. 3, different correlation times almost do not impose any significant difference on sensitivity to the speckle contrast when a certain exposure time of CCD camera is set. There exists a slight difference at the maximal peaks though, when the exposure time is extremely short. It theoretically affirms that the 2D distribution maps of the changes in blood flow from LSCI during a fixed exposure time will not be affected by the intrinsic correlation time of arteries, veins, or capillaries. However, if we choose different exposure times in LSCI to visualize the changes of CBF on the same imaged area, the resultant speckle contrast shows a strong dependence of the intrinsic correlation time of a single vascular unit as shown in Fig. 4. A shorter exposure time (less than 10 milliseconds) is more sensitive to the shorter correlation time. But, if the correlation time is long

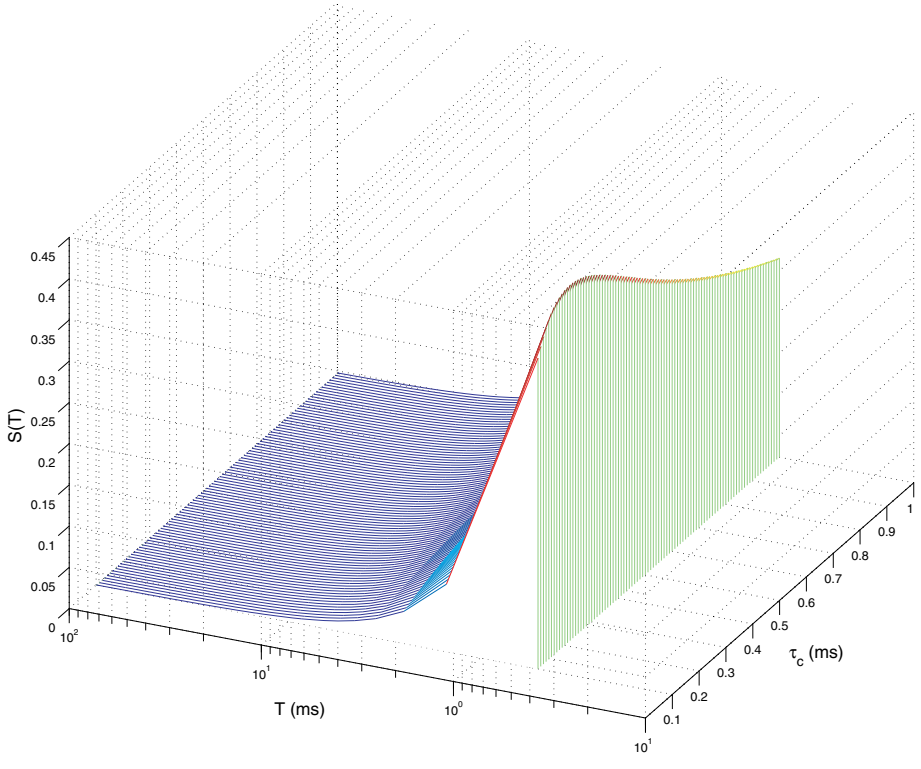

Fig. 4. Theoretical sensitivity function of parameter T. At a certain correlation time (suppose the imaged object is a single blood vessel with a stable correlation time), different exposure times clearly demonstrated distinct sensitivity to the changes in the speckle contrast.

approaching to 1 millisecond, a better sensitivity can be obtained theoretically around ∼10 milliseconds exposure time. This is in accordance with the previous conclusions since the smaller blood vessels have much better visibility in the speckle contrast images when using longer exposure time (20 milliseconds). (see Fig. 4 in Yuan *et al.*'s work[32]) This concept has been pushed forward to remove static speckle background and increase the sensitivity of the flow measurement by using a multi-exposure scheme.[33]

In most of the *in vivo* applications, relative changes of blood flow, usually, are used as one of the vital signs to assess the physiological status of the subjects. Following the approach of Yuan *et al.*,[32] the sensitivity analysis can also be done by making explicit the dependence of the speckle contrast on the change of blood flow with respect to the ratio, $r = \tau_c/T$, while the correlation time is believed to hold an inverse relationship with the blood velocity ($\tau_c \propto A/v$)[30]:

$$S(r) = \left|\frac{\frac{dC}{C}}{\frac{dv}{v}}\right| = \left|-\frac{r}{C}\cdot\frac{dC}{d(r)}\right| = \frac{(r+1)\exp(-2/r) - r + 1}{r\exp(-2/r) + 2 - r} \tag{11}$$

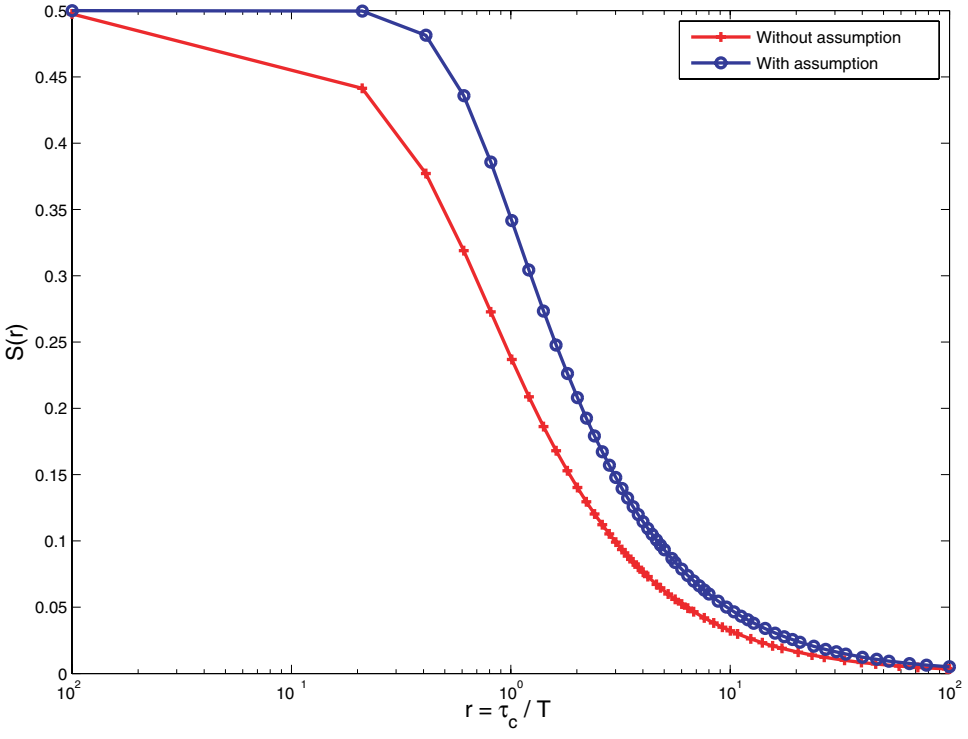

Fig. 5. Theoretical sensitivity function of relative velocity of blood flow against r, with/without the assumption $(1 - \frac{|\tau|}{T}) \approx 1$.

As shown in Fig. 5, the sensitivity curve shares very similar characteristics with the result from previous work.[32] Evidently, $S(r)$ almost reaches the maximal value when $T > 10\tau_c$ (i.e., $r < 10^{-1}$). Basically, one can choose an optimal exposure time based on the correlation time of the targeted blood flow. It is coherent with the conclusion that sub-millimeter functional-resolution imaging of blood flow in the neocortex can be achieved at relatively longer exposure time (20 milliseconds or slightly longer) in LSCI.[13] In other words, longer an exposure time is helpful to reveal more detailed microvascular structures. However, it should be borne in mind that too long an exposure time would cause temporal averaging to suppress speckle and also lose the advantages on temporal resolution.

4. Open Questions

In spite of its recent introduction to brain imaging,[10,11] the LSCI technique has inspired a rising wave of biomedical applications of monitoring changes in blood flow both under normal brain functional and diseased states. However, there remain many technical issues with regard to the performance of the tool, practical

considerations of working on animal model, and the interpretation of speckle contrast images.

4.1. *Static scattering*

Undoubtedly, the interference effect will form when the coherent light is scattered off a stationary surface as long as the surface is rough enough to create path-length difference exceeding a wavelength of the light. According to the diffraction theory, each point on an illuminated surface acts as a source of secondary spherical waves that have their own phases and amplitudes. The difference in optical path length induces phase changes greater than 2π, resulting in the random changes in the intensity of the scattered light. Due to this kind of static scattering, it roughly adds on a static speckle background to the dynamic speckle images acquired by using a LSCI setup. In 1997, Boas and Yodh developed a formalism to deal with the effect of static scattering that contaminates the dynamic scattering measurements,[34] which is recently applied by two other groups.[33,35] The basic idea assumes that the electric field reaching the detector consists of two components: photons that do not scatter with moving particles at all and photons that experience at least an interaction once with a moving particle. This treatment can be easily incorporated into the framework we advance by modifying the Siegert relation with two appropriate terms (see Eq. (15)[34]). More recently, Parthasarathy *et al.* took one step further to apply multi-exposure scheme to provide more robust detection on the flow.[33] However, this analytical formula introduces some complicating factors into the LSCI model and data acquisition. Future work needs to simplify this procedure in order to facilitate its application.[36] From this point of view, some sort of image post-processing may be a good candidate for solving this problem while preserving the technical simplicity of LSCI.[37] Another option is to combine two orthogonal polarization filters into the LSCI system. This arrangement can filter out specularly reflected photons, as the initial polarization state of these photons remains unchanged due to the very few times of scattering.[38]

4.2. *Biological zero*

It has long been recognized that there exists some kind of residual signal in the Laser Doppler Flowmetry (LDF) measurement from the tissue in the absence of vascular flow, called biological zero (BZ).[39] This "problem" is shared by LSCI measurement as well since it is inherent in photon-tissue interaction. Until now, however, it is not much appreciated by the investigators in the laser speckle field. The physiological sources of the BZ signal are fairly complicated. There are many factors such as changes in blood volume, hematocrit, temperature, and residual vasomotion that will exert significant influences on the BZ values obtained in experiments. It is commonly believed that BZ signal is considered primarily originating from Brownian motion — the random wandering movement of the moving blood cells.[39–42] Zhong *et al.* put forward an elegant mathematical treatment for solving this BZ problem in

LDF measurement.[42] They presumed that the speed composition of the moving red blood cells had two components: a random fluctuation caused by Brownian motion and a net global translational velocity. The speed distribution of the red blood cells in random movement can be described by the Maxwell–Boltzmann probability density distribution. As a matter of fact, what the classic Bonner–Nossal model has established is the linear relationship between the output of the LDF and the square root of the averaged squared speed, $\langle v^2 \rangle^{1/2}$, that is defined by the Maxwell–Boltzmann speed distribution (as plotted in Fig. 6).[30]

Based on the above assumption, $\langle v^2 \rangle^{1/2}$, to some extent, represents the desired translational speed with the shifted baseline due to the BZ component. Thus, a modified speed distribution function can take into account of these two components. As for the framework discussed in the paper, the strategy could be adopted by modifying the expression of $\mu_A(\tau)$, i.e., in Eq. (7). However, it is not a trivial work since characterization of $\mu_A(\tau)$ is empirically hard to accomplish. It depends on too many complicating factors such as the experimental setup (e.g. illumination condition), the cranial window created on the animal's head, and the physiological status of the animal. The current biophysical model is far from the settled position and needs further improvements.

Besides this, the functional significance of Brownian motion in perfused tissue is not clear. Consequently, it is premature to conclude whether the BZ signal

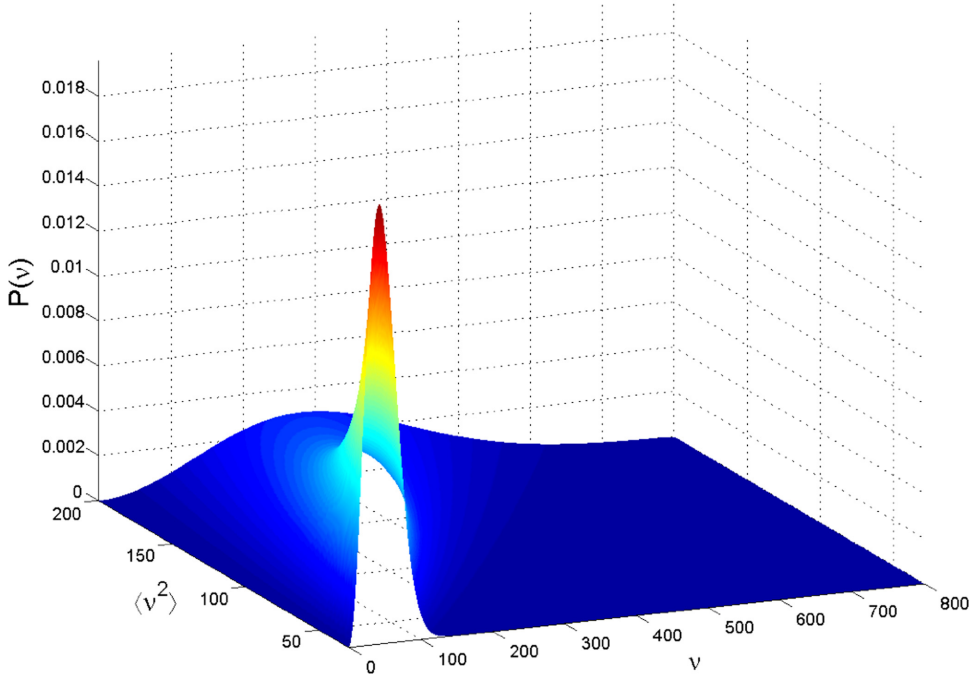

Fig. 6. A 3D plot of Maxwell–Boltzmann speed probability density distribution.

should be subtracted from the normal perfusion measurement unless the behavior of this Brownian motion is fully understood. Although the BZ's contribution to the LDF or LSCI output is small in most cases, this issue deserves more attention in terms of interpreting properly the underlying physiological responses reflected by the speckle images. Even for LDF technique that is considered as a gold-standard measurement of blood flow in clinical diagnostics, the BZ problem, somehow, is one of the major obstacles for a better performance.[40] More substantial work is required to be addressed in the future.

4.3. *Motion artifact*

Since LSCI exploits the spatial statistics properties of laser speckle to obtain the 2D velocity distribution through analyzing the spatial blurring of the raw speckle images, any other blurring effects due to unwanted movement artifacts could cause bias in estimating the relative changes of blood flow in experiments. This is really a problematic issue for animal imaging, in particular when the subjects are awake. In spite of the fact that the animal is anesthetized, the tissue or head motion generated by respiratory and cardiac systems of the body could completely change the speckle pattern from time to time. In the authors' laboratory, lots of efforts have been devoted to overcome this difficulty in order to implement LSCI on the awake primates. Since the range of such body motion is usually much larger than the coherent radius of a speckle, it is rather challenging to assess its influences and correct it from the resultant speckle images. If only the surface speckle pattern is affected by the body movement, it seems reasonable to count on the polarization state of the scattered light to eliminate it.[38] But, we will lose some photons that might encode the superficial flow information and then suffer a decreased signal-to-noise ratio (SNR).

4.4. *Phase noise*

Speckle is the resultant sum of a type of signal that consists of a multitude of independently-phased additive complex vectorial components.[20] The relative phases among these components will decide whether the final sum (speckle intensity) may be small or large. Obviously, any factors other than variations of blood flow that cause the transmitted photons in the tissue dephasing will confound the LSCI results. Broadly speaking, the aforementioned problems can all attribute to the concept of phase noise.

For a start, we considered the phase noise in laser source although this had not been given much attention so far. Due to the quantum noise or other technical noises (e.g. temperature fluctuation, vibration of the cavity mirrors) in the generation of laser, the output of a single frequency laser is not perfectly monochromatic, but rather exhibits some phase noise. Simply, it leads to a finite linewidth (mixture of different frequencies) of the laser output. Such laser light already loses some degree of coherence even before it enters into the tissue. It brings up several consequential

effects. First, the polychromatic speckle may not follow the statistics of Gaussian function and further violate the Siegert relation. Second, it was reported that geometrical factors cause the polychromatic speckle pattern contrast to decrease when the optical path-length differences are larger than the coherence length.[23] This will complicate the LSCI system setup including the size of the illuminated spot, the distances between the light source, the object, and the observation plane. Therefore, this is an important aspect of the technical issues when one begins to establish an LSCI system.

Taken together, various kinds of phase noises seriously deteriorate the SNR of the speckle images. Despite the fact that much efforts have been dedicated to the denoise scheme,[35,43] it will be helpful to present a unified view angle to reconsider these open questions.

4.5. *LSCI as analog of MRI*

In MRI field, phase-contrast methods have been widely used to measure blood flow for more than 20 years.[44–46] With regard to theoretical basis, the phase-contrast MRI shares many similar features with the LSCI. It is not surprising as they are situated at neighboring parts of the electromagnetic spectrum (wavelength: $\sim$10 m vs. $\sim$800 nm). The coherent spectroscopy began around 1950 with demonstration of the spin echo in nuclear magnetic resonance (NMR),[47] which used the well-defined amplitude and phase modulation of radiation field to extract information about atoms or molecules. At present, the spin echo has been popularly used to reverse the unwanted dephasing effects due to the field inhomogeneity and acquire T_2-weighted (transverse relaxation) MRI images. Later in 1956, Feynman *et al.* demonstrated a ground-breaking theory that all two-level systems are mathematically equivalent. They had visions of optical version of spin echo that if coherent light fields were created, it would be possible to implement the same methods on optical transition.[48] Indeed, the photon echo was realized soon after the invention of laser.[49]

In most of phase-contrast MRI methods, one always looks for the phase difference between the moving spins in the presence of magnetic-field gradients and the static spins. To achieve appropriate estimation of the phase contrast induced by the flow phenomenon, the incidental fluctuations in phase associated with field inhomogeneities or others irrelevant to flow have to be subtracted out. This compensation strategy can be combined with the use of complex radio frequency (RF) pulse and gradient sequences to gain more efficient phase-sensitive detection of the moving and static spins evolution. If some phase-controlled optical pulse sequences (e.g., femtosecond pulse-shaping technology[50]) can be generated thus allowing the corresponding electric field measurements to be made, then the convoluted phase processes of LSCI might be easily disentangled. It may also open a window for optical deep-tissue imaging with scattering effects suppressed. Conversely, bringing the power of modern optics to the MRI methodology could greatly improve its image resolution and sensitivity.[51] These two techniques have developed separately over

20 years or so. It is evident that not everyone in either field realizes that some merits of these two methods can be taken advantage of to improve flow measurements. This paper makes an initial attempt to build a conceptual link between LSCI and MRI and this cross-modality development undoubtedly holds out a vision of advancing both optical imaging and MRI technology in the future.

5. Conclusion

In summary, this paper has reviewed theoretical backgrounds of the LSCI technique, and presented a complete framework based on a simple biophysical model, and provided some instructive rules as to how to exercise this technique for practical applications. The discussion indicates that there is considerable room for optimizing this imaging technique. Some technical issues of immediate interest are raised for next-step study. In short, LSCI is a very promising method for achieving *in vivo* high-resolution (at tens of micrometer and millisecond level) visualization of changes in blood flow for both research purposes and clinical diagnostics in the nearest future. It can be anticipated as a complementary method to fill the gap between the two-photon imaging and fMRI technique.

Acknowledgments

This research work is funded by the Canadian Institutes of Health Research (CIHR) Strategic Training Program in Vascular Research.

References

1. Roy, C. S. and Sherrington, C. S., "On the regulation of the blood-supply of the brain," *J. Physiol.* **11**, 85–158 (1890).
2. Woolsey, T. A., Rovainen, C. M., Cox, S. B., Henegar, M. H., Liang, G. E., D. Liu, Moskalenko, Y. E., Sui, J. and Wei, L., "Neuronal units linked to microvascular modules in cerebral cortex: Response elements for imaging the brain," *Cereb. Cortex* **6**, 647–660 (1996).
3. Raichle, M. E., "Behind the scenes of functional brain imaging: A historical and physiological perspective," *Proc. Natl. Acad. Sci. USA* **95**, 765–772 (1998).
4. Iadecola, C., "Neurovascular regulation in the normal brain and in Alzheimer's disease," *Nat. Rev. Neurosci.* **5**, 347–360 (2004).
5. Lauritzen, M., "Reading vascular changes in brain imaging: Is dendritic calcium the key?," *Nat. Rev. Neurosci.* **6**, 77–85 (2005).
6. Harrison, R. V., Harel, N., Panesar, J. and Mount, R. J., "Blood capillary distribution correlates with hemodynamic-based functional imaging in cerebral cortex," *Cereb. Cortex* **12**, 225–233 (2002).
7. Kety, S. S. and Schmidt, C. F., "The determination of cerebral blood flow in man by the use of nitrous oxide in low concentrations," *Am. J. Physiol.* **143**, 53–67 (1945).
8. Chen, L. M., Heider, B., Williams, G. V., Healy, F. L., Ramsden, B. M. and Roe, A. W., "A chamber and artificial dura method for long-term optical imaging in the monkey," *J. Neurosci. Methods* **113**, 41–49 (2002).

9. Ayata, C., Dunn, A. K., Gursoy, O. Y., Huang, Z., Boas, D. A. and Moskowitz, M. A., "Laser speckle flowmetry for the study of cerebrovascular physiology in normal and ischemic mouse cortex," *J. Cereb. Blood Flow Metab.* **24**, 744–755 (2004).
10. Bolay, H., Reuter, U., Dunn, A. K., Huang, Z., Boas, D. A. and Moskowitz, M. A., "Intrinsic brain activity triggers trigeminal meningeal afferents in a migraine model," *Nat. Med.* **8**, 136–142 (2002).
11. Dunn, A. K., Bolay, H., Moskowitz, M. A. and Boas, D. A., "Dynamic imaging of cerebral blood flow using laser speckle," *J. Cereb. Blood Flow Metab.* **21**, 195–201 (2001).
12. Weber, B., Burger, C., Wyss, M. T., von Schulthess, G. K., Scheffold, F. and Buck, A., "Optical imaging of the spatiotemporal dynamics of cerebral blood flow and oxidative metabolism in the rat barrel cortex," *Eur. J. Neurosci.* **20**, 2664–2670 (2004).
13. Wang, Z., Hughes, S., Dayasundara, S. and Menon, R. S., "Theoretical and experimental optimization of laser speckle contrast imaging for high specificity to brain microcirculation," *J. Cereb. Blood Flow Metab.* **27**, 258–269 (2007).
14. Goodman, J. W., "Some effects of target-induced scintillations on optical radar performance," *Proc IEEE* **53**, 1688–1700 (1965).
15. Ohtsubo, J. and Asakura, T., "Velocity measurement of a diffuse object by using time-varying speckles," *Opt. Quant. Electr.* **8**, 523–529 (1976).
16. Takai, N., Iwai, T., Ushizaka, T. and Asakura, T., "Zero-crossing study on dynamic properties of speckles," *J. Opt. (Paris)* **11**, 93–101 (1980).
17. Fercher, A. F. and Briers, J. D., "Flow visualization by means of single-exposure speckle photography," *Opt. Commun.* **37**, 326–329 (1981).
18. Goodman, J. W., Statistical Properties of laser speckle patterns, in: J. C. Dainty, (ed.) *Laser Speckle and Related Topics* (Springer-Verlag, Berlin, 1975), pp. 9–75.
19. Goodman, J. W., *Statistical Optics* (Wiley, New York, 1985).
20. Goodman, J. W., *Speckle Phenomena in Optics: Theory and Applications* (Greenwood Village: Roberts & Company, 2006).
21. Jakeman, E., Photon correlation, in: H. Z. Cummings & E. R. Pike (eds.) *Photon Correlation and Light Beating Spectroscopy* (Plenum Press, London, 1973), pp. 75–149.
22. Gittings, A. S. and Durian, D. J., "Gaussian and non-Gaussian speckle fluctuations in the diffusing-wave spectroscopy signal of a coarsening foam," *Appl. Opt.* **45**, 2199–2204 (2006).
23. Markhvida, I., Tchvialeva, L., Lee, T. K. and Zeng, H., "Influence of geometry on polychromatic speckle contrast," *J. Opt. Soc. Am. A. Opt. Image. Sci. Vis.* **24**, 93–97 (2007).
24. Pries, A. R., Secomb, T. W. and Gaehtgens, P., "Biophysical aspects of blood flow in the microvasculature," *Cardiovasc. Res.* **32**, 654–667 (1996).
25. Stern, M. D., "*In vivo* evaluation of microcirculation by coherent light scattering," *Nature* **254**, 56–58 (1975).
26. Wang, L., Jacques, S. L. and Zheng, L., "MCML–Monte Carlo modeling of light transport in multi-layered tissues," *Comput. Methods Programs Biomed.* **47**, 131–146 (1995).
27. Briers, J. D., "Laser Doppler and time-varying speckle: A reconciliation," *J. Opt. Soc. Am.* **13**, 345–350 (1996).
28. Briers, J. D., Richards, G. and He, X. W., "Capillary blood flow monitoring using laser speckle contrast analysis (LASCA)," *J. Biomed. Opt.* **4**, 164–175 (1999).

29. Sokoloff, L., "Circulation in the central nervous system," in: R. Greger, & U. Windhorst (eds.) *Comprehensive Human Physiology* (Springer-Verlag, Berlin, 1996), pp. 561–578.
30. Bonner, R. and Nossal, R., "Model for laser Doppler measurements of blood flow in tissue," *Appl. Opt.* **20**, 2097–2107 (1981).
31. Attwell, D. and Iadecola, C., "The neural basis of functional brain imaging signals," *Trends Neurosci.* **25**, 621–625 (2002).
32. Yuan, S., Devor, A., Boas, D. A. and Dunn, A. K., "Determination of optimal exposure time for imaging of blood flow changes with laser speckle contrast imaging," *Appl. Opt.* **44**, 1823–1830 (2005).
33. Parthasarthy, A. B., Tom, W. J., Gopal, A., Zhang, X. and Dunn, A. K., "Robust flow measurement with multi-exposure speckle imaging," *Opt. Exp.* **16**, 1975–1989 (2008).
34. Boas, D. A. and Yodh, A. G., "Spatially varying dynamical properties of turbid media probed with diffusing temporal light correlation," *J. Opt. Soc. Am.* **14**, 192–215 (1997).
35. Zakharov, P., Volker, A., Buck, A., Weber, B. and Scheffold, F., "Quantitative modeling of laser speckle imaging," *Opt. Lett.* **31**, 3465–3467 (2006).
36. Cheng, H. and Duong, T. Q., "Simplified laser-speckle-imaging analysis method and its application to retinal blood flow imaging," *Opt. Lett.* **32**, 2188–2190 (2007).
37. Li, P., Ni, S., Zhang, L., Zeng, S. and Luo, Q., "Imaging cerebral blood flow through the intact rat skull with temporal laser speckle imaging," *Opt. Lett.* **31**, 1824–1826 (2006).
38. Groner, W., Winkelman, J. W., Harris, A. G., Ince, C., Bouma, G. J., Messmer, K. and Nadeau, R. G., "Orthogonal polarization spectral imaging: A new method for study of the microcirculation," *Nat. Med.* **5**, 1209–1212 (1999).
39. Tenland, T., Salerud, E. G., Nilsson, G. E. and Oberg, P. A., "Spatial and temporal variations in human skin blood flow," *Int. J. Microcirc. Clin. Exp.* **2**, 81–90 (1983).
40. Binzoni, T., Leung, T. S., Seghier, M. L. and Delpy, D. T., "Translational and Brownian motion in laser-Doppler flowmetry of large tissue volumes," *Phys. Med. Biol.* **49**, 5445–5458 (2004).
41. Kernick, D. P., Tooke, J. E. and Shore, A. C., "The biological zero signal in laser Doppler fluximetry — origins and practical implications," *Pflugers Arch.* **437**, 624–631 (1999).
42. Zhong, J., Seifalian, A. M., Salerud, G. E. and Nilsson, G. E., "A mathematical analysis on the biological zero problem in laser Doppler flowmetry," *IEEE Trans. Biomed. Eng.* **45**, 354–364 (1998).
43. Volker, A. C., Zakharov, P., Weber, B., Buck, F. and Scheffold, F., "Laser speckle imaging with active noise reduction scheme," *Opt. Exp.* **13**, 9782–9787 (2005).
44. Dumoulin, C. L., Souza, S. P., Walker, M. F. and Wagle, W., "Three-dimensional phase contrast angiography," *Magn. Reson. Med.* **9**, 139–149 (1989).
45. Nishimura, D. G., Macovski, A. and Pauly, J. M., "Magnetic resonance angiography," *IEEE Trans. Med. Imaging* **5**, 140–151 (1986).
46. Pelc, N. J., Bernstein, M. A., Shimakawa, A. and Glover, G. H., "Encoding strategies for three-direction phase-contrast MR imaging of flow," *J. Magn. Reson. Imaging* **1**, 405–413 (1991).
47. Hahn, E., "Spin echoes," *Phys. Rev.* **80**, 580–594 (1950).
48. Feynman, R. P., Vernon, F. L. and Hellwarth, R. W., "Geometrical representation of the Schrodinger equation for solving maser problems," *J. Appl. Phys.* **28**, 49–52 (1957).

49. Kurnit, N. A., Abella, I. D. and Hartmann, S. R., "Photon echoes," *Phys. Rev. Lett.* **13**, 567–570 (1964).
50. Tian, P., Keusters, D., Suzaki, Y. and Warren, W. S., "Femtosecond phase-coherent two-dimensional spectroscopy," *Science* **300**, 1553–1555 (2003).
51. Savukov, I. M., Lee, S. K. and Romalis, M. V., "Optical detection of liquid-state NMR," *Nature* **442**, 1021–1024 (2006).